Struct Multidisc Optim (2009) 37:509–519
DOI 10.1007/s00158-008-0245-4

RESEARCH PAPER

Control–structural design optimization for vibration of piezoelectric intelligent truss structures

Guozhong Zhao · Biaosong Chen · Yuanxian Gu

Received: 1 September 2006 / Revised: 28 December 2007 / Accepted: 6 February 2008 / Published online: 4 July 2008

Abstract Based on the design sensitivity analysis for structural dynamics in time domain, an integrated control–structural design optimization method is proposed to the vibration control of piezoelectric intelligent truss structure. In this investigation, the objective function and constraint functions include not only the conventional design indexes of structure but also the vibration control indexes and the feedback control variables. The structural design variables are optimized simultaneously with the vibration control system. The sensitivity relations for the control–structure optimization model are derived by using a new method, and the sequential linear programming algorithm is used to solve this kind of optimization problem. The numerical examples given in the paper demonstrate the effectiveness of methods and the program.

Keywords Vibration control · Piezoelectric truss · Sensitivity analysis · Design optimization

1 Introduction

Space structures are usually lightly and weakly damped. Therefore, it is proper to make use of intelligent structures to actively control the vibration of space structures. The piezoelectric materials, as an important part of intelligent structural materials, have not only the ability of carrying load but also the mechanical–electric-coupling property and hence can serve as an actuator and a sensor. The researches on the numerical analysis of static and dynamic responses, and the vibration control of the piezoelectric intelligent structures have attracted more and more attention. For example, Tzou and Gadre (1989) proposed a multilayered thin shell with an active distributed vibration actuator. Ray et al. (1994) developed an eight-node brick piezoelectric element considering three-dimensional incompatible modes. A number of finite element models were given for comprehensive modeling of smart structures with segmented piezoelectric sensing and actuating patches by Sze and Yao (2000). Yang and Ngoi (2000) analytically addressed the formulation of the shape control of beams by piezoelectric actuators. Chen et al. (2002) used a simple negative velocity feedback control algorithm to actively control the dynamic response of the beam through a closed control loop. Kang et al. (2002) investigated the interaction between active and passive vibration control characteristics for carbon_epoxy laminated composite beams with a collocated piezoceramic sensor and actuator. Hwu et al. (2004) designed an observed-state feedback control system for the composite sandwich beams with surface bonded piezoelectric sensors and actuators by combining the present vibration analysis with the classical optimal control method. Lin and Nien (2005) investigated the modeling and vibration control of a smart beam using piezoelectric damping-modal actuators–sensors.

On the other hand, because the simultaneous design optimization of structures and control systems can result in both minimum weight and the control effort, this aspect has become an active research field in Miler and Shim (1987), Rao et al. (1988), Grandhi (1989), and Wang et al. (1999). According to the different methods

G. Zhao (✉) · B. Chen · Y. Gu
State Key Laboratory of Structural Analysis for Industrial Equipment, Department of Engineering Mechanics, Dalian University of Technology, Dalian 116024, China
e-mail: Zhaogz@dlut.edu.cn

by which the control gain variables and structural design variables are determined, the design optimization models of control-augmented structural synthesis can be classified into two kinds. The first approach is that the feedback gains are dependent on the structural design variables, and the control gains are solved from the Riccati equation. The second approach is that the structural design variables and control gains are treated as independent design variables. For example, Grandhi (1989) investigated the design optimization of the structure and control system with structural weight or Frobenious norm as the objective function and constraints on the closed-loop eigenvalue and the damping parameters with the first approach. Wang et al. (1999) optimized the structural element sizes and the feedback gains of intelligent structure considering the performance index of vibration control and the structural mass as objective functions with the second approach. It is known that the second approach is more reasonable to solve simultaneously the problems of control and structural optimization. Because of the mechanical–electric-coupling effect and the application of the feedback control theory, the design of the piezoelectric intelligent structures is more complicated than structures composed of conventional materials. In this paper, the second approach is employed to solve the problem of integrated optimization of structure and control system of piezoelectric intelligent truss structures.

Although some investigations in the optimization of control–structure designs have been done, very few work about the sensitivity analysis for piezoelectric truss system can be found in the literature. The numerical methods for design optimization and sensitivity analysis in control integrated with structural optimization for piezoelectric intelligent truss structures are studied in this paper. Firstly, based on the mechanical–electric-coupling effect, a finite element formulation for the analysis of intelligent structure with piezoelectric active bars is presented, and the direct output feedback control law is employed to suppress the structural vibration. Then, an optimization procedure for the simultaneous control–structure design is proposed. In this formulation, the design variables are not only the conventional variable of structural elements such as the cross-sectional areas of bars but also include the design parameters of control such as feedback control gains. The design constraints considered also include both structural behaviors and vibration control performance indices. The sequential linear programming (SLP) algorithm is used to solve the optimization problem, and the sensitivity analysis is carried out for objective and constraint functions to make linear approximations. Based on the Newmark integration method in time domain for the transient dynamic responses of structure, a new sensitivity analysis method is proposed. The numerical examples of sensitivity analysis and design optimization with various kinds of design variables are given to demonstrate the effectiveness of the methods.

2 Finite element model for piezoelectric intelligent trusses

It is a special property that the mechanical and the electrical effects are coupled in the piezoelectric elasticity. If we ignore the magnetic effect and thermal piezoelectric effect, the constitutive equations of piezoelectric materials with the linear mechanical–electric-coupling effect can be expressed by Sun and Zhang (1984)

$$\begin{aligned} \sigma &= c^{\mathrm{E}}\varepsilon - \boldsymbol{eE} \\ \boldsymbol{D} &= \boldsymbol{e}^{\mathrm{T}}\varepsilon + \Xi^{\varepsilon}\boldsymbol{E} \end{aligned} \tag{1}$$

where the σ is the stress vector, $\boldsymbol{D}$ the electric displacement vector, C^E the elastic constant matrix, $\boldsymbol{e}$ the piezoelectric coefficient matrix, Ξ^{ε} permittivity constant matrix on clip condition, ε the strain vector, and $\boldsymbol{E}$ the electric field vector.

The piezoelectric bar studied here is made of piezoelectric thin pieces shown in Fig. 1, where Φ is the electrical potential difference between the two surfaces of the electrical thin piece, t the thickness of the piezoelectric thin piece, L the length of the piezoelectric bar, N_1 and N_2 the axial forces. While the electrical voltage is given along the axial direction, the piezoelectric thin pieces will induce axial deformation and strain and hence the equivalent electrical force in axial direction. Therefore, the quantities $\boldsymbol{e}$ and Ξ^{ε} in (1) can be simplified to the e_{33} and Ξ^{ε}_{33}.

Multiplying (1) by the cross-sectional area of the bar and considering the equilibrium equations of the force and electricity, the following equations can be obtained

$$\begin{aligned} N &= (c_{33}A/L)\Delta u - (e_{33}A)/t)\Phi \\ Q &= ((e_{33}A)/t)\Delta u + ((n\Xi^{\varepsilon}_{33}A)/t)\Phi \end{aligned} \tag{2}$$

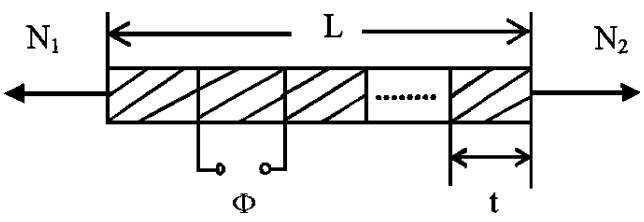

Fig. 1 The piezoelectric bar composed of the thin pieces

where, A is the cross-sectional area of bar, Δu the relative displacement between two nodes, $n = L/t$ the number of piezoelectric thin pieces of a bar and Q the electric charge.

According to the principles of the nodal force equilibrium and the electric charge equilibrium, considering the inertia force induced by the acceleration, the transformation of (2) from local coordinates into global coordinates yields the following equilibrium equations of the force and electric charge in the global coordinate system

$$\boldsymbol{P}^{\mathrm{e}} - M^{e}\ddot{\boldsymbol{u}}^{\mathrm{e}} = \lambda^{\mathrm{T}}\boldsymbol{K}_1 B\lambda u^{\mathrm{e}} + \lambda^{\mathrm{T}}\boldsymbol{K}_2\boldsymbol{\Phi}^{\mathrm{e}} \tag{3}$$

$$\boldsymbol{Q}^{\mathrm{e}} = \boldsymbol{K}_2^{\mathrm{T}}\boldsymbol{B}\lambda\boldsymbol{u}^{\mathrm{e}} + \lambda^{\mathrm{T}}\boldsymbol{K}_3\boldsymbol{\Phi}^{\mathrm{e}} \tag{4}$$

$$\boldsymbol{K}_1 = \left(C_{33}A/L\right) I,\ \ \boldsymbol{K}_2 = \left(e_{33}A/t\right) I,$$

$$\boldsymbol{K}_3 = \left(L\Xi_{33}^{\varepsilon}A/t^2\right) I,\ \ B = \begin{bmatrix} 1 & -1 \\ -1 & 1 \end{bmatrix} \tag{5}$$

where I is the 2×2 identity matrix, $\boldsymbol{P}^{\mathrm{e}}$ the mechanical load vector, M^{e} the mass matrix, $\boldsymbol{u}^{\mathrm{e}}$ the displacement vector, $\ddot{\boldsymbol{u}}^{\mathrm{e}}$ the acceleration vector, $\boldsymbol{\Phi}^{\mathrm{e}}$ the vector of the electric potential difference, λ the coordinate translation matrix, $\boldsymbol{Q}^{\mathrm{e}}$ the electric charge vector. Notice that all of these vectors and matrices can be determined in each element.

The global dynamics equation of piezoelectric truss can be derived from (3) and (4) by assembling all the elements and using the Guyan condensation (Guyan 1965) to eliminate the electrical potential vector

$$\boldsymbol{M}\ddot{\boldsymbol{u}} + (\boldsymbol{K} + K_{\mathrm{E}})\,\mathbf{u} = \boldsymbol{P} + K_{\mathrm{q}}Q \tag{6}$$

The (6) is different from that of the structures made of conventional materials. Here, the differences are additional mechanical–electric-coupling stiffness matrix K_{E} and an electric load vector $\boldsymbol{K}_q\boldsymbol{Q}$, where $\boldsymbol{K}$, K_{E}, and $\boldsymbol{K}_{\mathrm{q}}$ are obtained by assembling all the elements matrices K^{e}, $K_{\mathrm{E}}^{\mathrm{e}}$ and $K_{\mathrm{q}}^{\mathrm{e}}$. These matrices can be respectively described as

$$K^{\mathrm{e}} = \lambda^{\mathrm{T}}\boldsymbol{K}_1 B\lambda,\quad K_{\mathrm{E}}^{\mathrm{e}} = \frac{e_{33}^2 A}{\boldsymbol{L}\Xi_{33}^{\varepsilon}}\lambda^{\mathrm{T}}B\lambda \tag{7}$$

$$K_{\mathrm{q}}^{\mathrm{e}} = \lambda^{\mathrm{T}}\left(\frac{e_{33}t}{\boldsymbol{L}\Xi_{33}^{\varepsilon}}\right) I \tag{8}$$

Additionally, each piezoelectric thin piece can be considered as the parallel plate capacitor, and then the relationship between the electric charge $\boldsymbol{Q}$ and electric voltage $\boldsymbol{V}$ can be obtained as such

$$\boldsymbol{Q} = \mathrm{diag}\,\{c_1 c_2 \ldots c_m\}\,\boldsymbol{V} = \boldsymbol{C}\boldsymbol{V}\quad c_j = n_j\boldsymbol{\Xi}_{33}^{\varepsilon}A_j/t \tag{9}$$

where c_j, n_j, and A_j are respectively the capacity parameter, the numbers of piezoelectric thin pieces, the cross-sectional area for the jth piezoelectric bar, and m the number of piezoelectric bars for the truss system.

3 Vibration control for piezoelectric intelligent truss structures

In the piezoelectric intelligent truss structures, the sensors can be built into the active piezoelectric bars to measure the changes of the lengths for the active piezoelectric bars. When the control system amplifies the measuring information by using the feedback control law, the control voltage for the active bars can be determined, and the closed-loop feedback control is realized. For a collocated direct output feedback control law, the control voltage can be described as below

$$V_j = -h_j d - g_j\dot{d} \tag{10}$$

where h_j and g_j are the feedback gains to the relative displacement d and velocity $\dot{d}$ of the two ends for the jth piezoelectric active bars, respectively.

Substituting (10) into (9) and (6), the governing equations of the closed-loop control system can be obtained

$$\boldsymbol{M}\ddot{\boldsymbol{u}} + \boldsymbol{C}_{\mathrm{g}}\dot{\boldsymbol{u}} + (\boldsymbol{K} + \boldsymbol{K}_{\mathrm{E}} + \boldsymbol{K}_{\mathrm{h}})\,u = P \tag{11}$$

It is shown in (11) there are additional stiffness matrix $\boldsymbol{K}_{\mathrm{h}}$ and damping $\boldsymbol{C}_{\mathrm{g}}$ after applying the feedback control law, where $\boldsymbol{C}_{\mathrm{g}}$ and $\boldsymbol{K}_{\mathrm{h}}$ are assembled by elements matrices $\boldsymbol{C}_{\mathrm{g}}^{\mathrm{e}}$, $\boldsymbol{K}_{\mathrm{h}}^{\mathrm{e}}$. These matrices can be respectively described as

$$\boldsymbol{K}_{\mathrm{h}}^{\mathrm{e}} = h_j c_j\lambda^{\mathrm{T}}\boldsymbol{K}_{\mathrm{q}}^{\mathrm{e}}\boldsymbol{B}\lambda,\ \ \boldsymbol{C}_{\mathrm{g}}^{\mathrm{e}} = g_j c_j\lambda^{\mathrm{T}}\boldsymbol{K}_{\mathrm{q}}^{\mathrm{e}}\boldsymbol{B}\lambda \tag{12}$$

The (12) can be solved with the Newmark time integration method.

4 Design optimization model and solution algorithms

In this investigation, the objective function and constraint functions not only include the conventional functions in the structure dynamic optimization, such as the structural weight, the transient dynamic displacement, velocity, and acceleration but also include the electric voltage and control energy consumption. The design variables of the optimization model are of two categories of size variables (cross-sectional areas of bars) and the feedback control gains (displacement feedback gain coefficient and velocity feedback gain

coefficient). Then, the optimization formulation can be expressed as

$$\begin{cases} Find\ \{A_i, h_i, g_i\} \\ \min.\ J \\ S.t.\ \ J_{\mathrm{w}} \le \bar{\mathrm{J}}_{\mathrm{w}} \qquad J_{\mathrm{d}} \le \bar{\mathrm{J}}_{\mathrm{d}} \quad J_{\mathrm{v}} \le \bar{J}_{\mathrm{v}} \\ \quad u_i(t) \le \bar{\mathrm{u}} \qquad \dot{u}_i(t) \le \bar{\dot{\mathrm{u}}} \quad \ddot{u}_i(t) \le \bar{\ddot{\mathrm{u}}} \\ \quad V(t) \le \bar{\mathrm{V}} \\ \quad \underline{\mathrm{A}_i} \le A_i \le \overline{\mathrm{A}_i} \qquad \underline{\mathrm{g}_i} \le g_i \le \overline{\mathrm{g}_i} \ \ \underline{\mathrm{h}_i} \le h_i \le \overline{\mathrm{h}_i} \end{cases} \tag{13}$$

where $u_i(t), \dot{u}_i(t), \ddot{u}_i(t)$ are respectively the transient displacement, velocity, and acceleration of the ith degree of freedom. J_{w} is the structural weight, J_{d} and J_{v} can be described as

$$J_{\mathrm{d}} = \sum_{i=1}^{\mathrm{nd}} \int_{\mathrm{t_0}}^{\mathrm{t_f}} |u_i(t)| \mathrm{d}t, \quad J_{\mathrm{v}} = \sum_{k=1}^{m} \int_{\mathrm{t_0}}^{\mathrm{t}_f} |V_k(t)| \mathrm{d}t \tag{14}$$

where nd is the number of the structure degree of freedom, m the number of piezoelectric bars, $\mathrm{t_0}$ and t_f are respectively the initial time and final time. In this paper, J_{w} is the conventional structural cost performance, J_{d} is the structural vibration control performance and, J_{v} is the control energy consumption performance. The objective function J can take the form as

$$J \in (J_{\mathrm{d}}, J_{\mathrm{v}}, J_{\mathrm{w}}) \tag{15}$$

The (15) means the objective function J is J_{d}, J_{v}, or J_{w}. When one of these performances is selected as objective function, the other two performances are constraint functions.

The solution algorithm for the optimization problem (14) is the improved SLP. In the SLP algorithm (Wang 1991; Lamberti and Pappalettere 2004), the objective and constraint functions are approximated with linear extensions at the current design point during the optimization iteration. Then the original problem (13) is transformed into the following linear programming problem.

$$\begin{cases} min\ J(x_0) + \nabla^{\mathrm{T}} J(x_0)\, \Delta x \\ s.t.\ G_j(x_0) + \nabla^{\mathrm{T}} G_j(x_0)\, \Delta x \le 0 \qquad j = (1, 2, \ldots\ldots, m) \\ x_{i\mathrm{L}} \le x_i \le x_{i\mathrm{U}} \qquad i = (1, 2, \ldots\ldots, n) \end{cases} \tag{16}$$

where x is the design variable, x_0 the current design point, n the number of design variables x_i, m the number of constraint functions $G_j(x)$, and x_{iU} and x_{iL} the upper and the lower bounds of design variables. The $\nabla^T J(x_0)$ and $\nabla^T G_j(x_0)$ are derivative gradients of the objective function and constraint functions, respectively. The linear programming problem (16) is solved with the Lamke pivot algorithm (Bazaraa and Shetty 1979) to find a new design. This procedure is repeated until the convergence is reached.

In the improved SLP (Gu et al. 1998), in order to deal with the numerical error problem induced in the linear approximation of constraint functions and ensure optimization iteration converge, the numerical approaches of the approximate line search, the adaptive move limit, and the constraint relaxation have been employed.

The design optimization procedures are outlined below:

1. Solution of vibration control equation of piezoelectric truss structures;
2. Generation of optimization model;
3. Solution of sensitivity analysis;
4. Solution of optimum model with SLP based on the results of finite element model analysis and sensitivity analysis;
5. If convergence is reached, then stop; otherwise return to (1).

In the second step, it is important to determine values of all the constraint functions and objective function. But the maximum displacement, velocity, and acceleration are the time-dependent constraints. Therefore, the instant time, when the maximum displacement, velocity, or acceleration occurs, varies during the iteration process. But the calculation of their sensitivities is based on the instant time. It means if the instant changes in the next iteration step, sensitivity of the transient constraint is invalid in the current iteration step. In order to improve the stability of the iterations, not only the instant of the largest constraint but also the instants of several largest constraints are searched. When optimization model is solved with SLP, sensitivities of these concerned instants will be considered as the gradients of the constraint functions. The number of the sensitivities needed is dependent on the complexity of the structure configuration and optimization model. The more complicated the structure and optimization model are, the more sensitivities are needed.

5 Sensitivity analysis method

Because the derivatives of the weight J_{w} are the same as the conventional structures, here we only discuss the derivatives of the other constraints. In order to get the sensitivity of J_{d} and J_{v}, the time domain is divided into the following three parts:

$$\begin{cases} \text{When}\ \ u_i(t) < 0, \quad t \in (\mathrm{t_0} \sim \mathrm{t_1}) \\ \text{When}\ \ u_i(t) = 0, \quad t \in (\mathrm{t_1} \sim \mathrm{t_2}) \\ \text{When}\ \ u_i(t) > 0, \quad t \in (\mathrm{t_2} \sim \mathrm{t_f}) \end{cases} \tag{17}$$

Then, we have the following sensitivity formulation for J_d

$$\frac{\partial J_d}{\partial x_i} = \sum_{i=1}^{nd} \int_{t_0}^{t_1} \left(-\frac{\partial u_i(t)}{\partial x_i} \right) dt + \sum_{i=1}^{nd} \int_{t_1}^{t_2} \left| \frac{\partial u_i(t)}{\partial x_i} \right| dt + \sum_{i=1}^{nd} \int_{t_2}^{t_f} \frac{\partial u_i(t)}{\partial x_i} dt \quad (18)$$

It is obvious that we can obtain the sensitivities of J_v with the same method. From (14) and (18), it is noticed that the sensitivities of the all constraints are dependent on the derivatives of the time-varying displacement, velocity, acceleration, and voltage. Therefore, the attention should be paid to their sensitivity first.

Differentiating (11) and (10) with respect to the design variable at each element gives

$$\boldsymbol{M}\frac{\partial \ddot{\boldsymbol{u}}}{\partial x_i} + \boldsymbol{C}_g\frac{\partial \dot{\boldsymbol{u}}}{\partial x_i} + (\boldsymbol{K}+\boldsymbol{K}_E)\frac{\partial \boldsymbol{u}}{\partial x_i} = \frac{\partial \boldsymbol{p}}{\partial x_i} - \frac{\partial \boldsymbol{M}}{\partial x_i}\boldsymbol{u} - \left(\frac{\partial \boldsymbol{K}}{\partial x_i} + \frac{\partial \boldsymbol{K}_E}{\partial x_i} + \frac{\partial \boldsymbol{K}_h}{\partial x_i}\right)\boldsymbol{u} - \frac{\partial \boldsymbol{C}_g}{\partial x_i}\dot{\boldsymbol{u}} \quad (19)$$

$$\frac{\partial V_j}{\partial x_i} = -\frac{\partial h_j}{\partial x_i}d - h_j\frac{\partial d}{\partial x_i} - \frac{\partial g_j}{\partial x_i}\dot{d} - g_j\frac{\partial \dot{d}}{\partial x_i} \quad (20)$$

The (19) is the same type as that of (12) and can be solved with the same procedure to get the sensitivities of displacement, velocity, and acceleration. Furthermore, when (11) and (19) are solved, the decomposition of the matrix, which appears in the left hand of (11) and (19), is needed only once. The derivatives of the relative displacement and velocity in the (20) can be taken from (19). Therefore, it can be found that the sensitivities of the dynamic response and the control voltage are dependent on the derivatives of $\boldsymbol{M}$, $\boldsymbol{C}_g$, $\boldsymbol{K}$, $\boldsymbol{K}_E$, and $\boldsymbol{K}_h$. Because the derivatives of the elastic stiffness matrix and mechanical load vector are the same as the conventional material structures, we discuss here only how to compute the derivatives of $\boldsymbol{C}_g$, $\boldsymbol{K}_E$, and $\boldsymbol{K}_h$.

The derivatives of global matrices in (19) can be obtained by assembling all elements' matrix derivatives. By differentiating (7) and (12) with respect to the design variable at each element, the element matrix derivatives are expressed as

$$\frac{\partial \boldsymbol{K}_E^e}{\partial x_i} = \frac{\partial\left(\left(e_{33}^2 A_j\right)/(L\Xi_{33})\right)}{\partial x_i}\lambda^T\boldsymbol{B}\lambda \quad (21)$$

$$\frac{\partial}{\partial x_i}\boldsymbol{K}_{h_j}^e = \lambda^T\left(\frac{\partial c_j}{\partial x_i}\boldsymbol{K}_{q_j}^e h_j\boldsymbol{B} + \frac{\partial K_{q_j}^e}{\partial x_i}c_j h_j\boldsymbol{B} + \frac{\partial h_j}{\partial x_i}\boldsymbol{K}_{q_j}^e c_j\boldsymbol{B}\right)\lambda \quad (22)$$

$$\frac{\partial}{\partial x_i}\boldsymbol{C}_{g_j}^e = \lambda^T\left(\frac{\partial c_j}{\partial x_i}\boldsymbol{K}_{q_j}^e g_j\boldsymbol{B} + \frac{\partial \boldsymbol{K}_{q_j}^e}{\partial x_i}c_j g_j\boldsymbol{B} + \frac{\partial g_j}{\partial x_i}\boldsymbol{K}_{q_j}^e c_j\boldsymbol{B}\right)\lambda \quad (23)$$

For the size design variables, (22) and (23) can be simplified as

$$\frac{\partial}{\partial x_i}\boldsymbol{K}_{h_j}^e = \lambda^T\left(\frac{\partial c_j}{\partial x_i}\boldsymbol{K}_{q_j}^e h_j\boldsymbol{B} + \frac{\partial \boldsymbol{K}_{q_j}^e}{\partial x_i}c_j h_j\boldsymbol{B}\right)\lambda \quad (24)$$

$$\frac{\partial}{\partial x_i}\boldsymbol{C}_{g_j}^e = \lambda^T\left(\frac{\partial c_j}{\partial x_i}K_{q_j}^e g_j\boldsymbol{B} + \frac{\partial \boldsymbol{K}_{q_j}^e}{\partial x_i}c_j g_j\boldsymbol{B}\right)\lambda \quad (25)$$

Where $\partial \boldsymbol{K}_{q_j}^e/\partial x_i$ and $\partial c_j/\partial x_i$ can be obtained by differentiating (8) and (9)

$$\frac{\partial \boldsymbol{K}_{q_j}^e}{\partial x_i} = 0,\quad \frac{\partial c_j}{\partial x_i} = \frac{\partial}{\partial x_i}\left(n_j\Xi_{33}A_j/t\right) \quad (26)$$

For the displacement feedback gain design variables, (22) and (23) can be simplified as

$$\frac{\partial}{\partial x_i}K_{h_j}^e = \lambda^T c_j K_{q_j}^e B\lambda,\quad \frac{\partial}{\partial x_i}C_{g_j}^e = 0 \quad (27)$$

For the velocity feedback gains design variables, (22) and (23) can be simplified as the following

$$\frac{\partial}{\partial x_i}\boldsymbol{C}_{g_j}^e = \lambda^T c_j\boldsymbol{K}_{q_j}^e\boldsymbol{B}\lambda,\quad \frac{\partial}{\partial x_i}\boldsymbol{K}_{h_j}^e = 0 \quad (28)$$

Therefore the derivatives of all the matrices in (19) have been obtained and the sensitivities of the displacement, velocity, and acceleration can be taken by solving (19). Substituting the derivatives of the displacement and velocity into (20), the derivative of the transient voltage is also obtained. Then from (18), we can also obtain the derivatives of J_d and J_v. Now all the sensitivities of the constraints with respect to design variables have been determined and the integrated structure and control optimization problem in (13) can be solved with SLP.

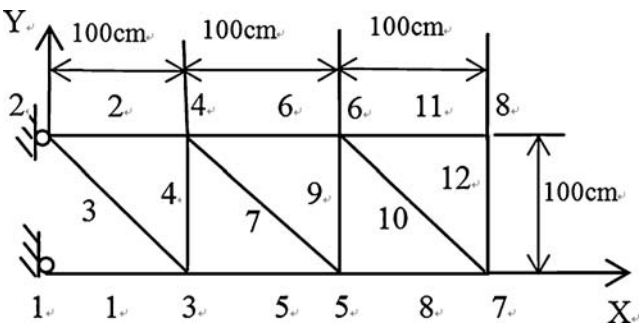

Fig. 2 Twelve-bar piezoelectric truss

Table 1 The sensitivities with size design variables (dA = 1.0E-7 m^2)

Design variable	Maximum displacement		Maximum voltage	
	FDM	SAM	FDM	SAM
A_1	1.0190	1.0192	−1.9269E5	−1.9274E5
A_2	6.5630E-1	6.5650E-1	−1.2989E5	−1.2993E5
A_3	−7.2110E-2	−7.2149E-2	9.9852E5	9.9874E5
A_4	1.3050E-2	1.3049E-1	−3.1410E3	−3.1411E4
A_5	7.7127E-1	7.7145E-1	−3.6708E4	−3.6724E4
A_6	3.1486E-1	3.1490E-1	−9.6876E4	−9.6916E4
A_7	5.8954E-1	5.8963E-1	−1.3287E5	−1.3291E5
A_8	3.7100E-1	3.7103E-1	1.0051E5	1.0052E5
A_9	4.4039E-1	4.4044E-1	−7.3020E3	−7.3050E3
A_{10}	6.0228E-1	6.0236E-1	3.1737E5	3.1742E5
A_{11}	2.1678E-1	2.1677E-1	1.3444E5	1.3445E5
A_{12}	2.4006E-1	2.4004E-1	2.3523E5	2.3524E5

Table 2 The sensitivities with displacement feedback gain coefficient variables (dh = 1.0E2)

Design variable	Maximum displacement		Maximum voltage	
	FDM	SAM	FDM	SAM
h_1	5.8400E-12	5.8371E-12	−1.0938E-6	−1.0938E-6
h_2	3.7300E-12	3.7318E-12	−7.5660E-7	−7.5660E-7
h_3	−1.2100E-12	−1.2151E-12	−7.6286E-5	−7.6286E-5
h_4	1.7000E-13	1.6300E-13	−1.4771E-7	−1.4771E-7
h_5	3.4900E-12	3.4917E-12	−1.0574E-7	−1.0574E-7
h_6	7.5000E-13	7.4413E-13	−7.2304E-7	−7.2304E-7
h_7	2.3400E-12	2.3361E-12	−8.8669E-7	−8.8669E-7
h_8	7.1000E-13	7.0833E-13	1.9367E-7	1.9367E-7
h_9	8.3000E-13	8.2608E-13	8.0331E-9	8.0332E-9
h_{10}	2.2900E-12	2.2915E-12	1.1248E-6	1.1248E-6
h_{11}	0.0000E+00	−5.4594E-15	−5.7549E-9	−5.7549E-9
h_{12}	4.4000E-13	4.3800E-13	2.0147E-7	2.0147E-7

Table 3 The sensitivities with velocity feedback gain coefficient variables (dg = 1.0)

Design variable	Maximum displacement		Maximum voltage	
	FDM	SAM	FDM	SAM
g_1	3.5420E-09	3.5416E-9	−8.1091E-4	−8.1094E-4
g_2	5.7100E-10	5.7063E-10	7.6295E-5	7.6303E-5
g_3	2.1000E-10	2.1001E-10	−7.2395E-2	−7.2396E-2
g_4	3.8100E-10	3.8074E-10	8.0554E-4	8.0555E-4
g_5	9.5000E-10	9.4984E-10	1.1930E-3	1.1930E-3
g_6	−3.6300E-10	−3.6337E-10	6.0859E-4	6.0863E-4
g_7	1.6260E-9	1.6254E-9	1.6133E-3	1.6134E-3
g_8	−2.0900E-10	−2.0956E-10	1.2260E-4	1.2253E-4
g_9	2.6500E-10	2.6511E-10	−1.0201E-4	−1.0203E-4
g_{10}	−4.5100E-10	−4.5118E-10	1.9336E-3	1.9336E-3
g_{11}	2.7000E-11	2.6354E-11	−1.9759E-4	−1.9760E-4
g_{12}	−1.8900E-10	−1.8931E-10	−7.5747E-4	−7.5754E-4

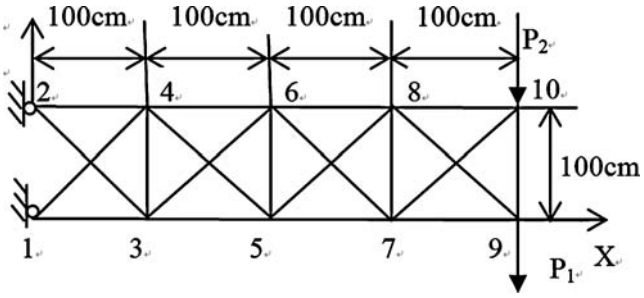

Fig. 3 Twenty-bar piezoelectric truss

6 Numerical examples

The above formulations and methods are implemented and a program is developed with C code. The following three examples are computed in Pentium 4 personal computer with 2.4 G central processing unit (CPU) speed.

6.1 Example 1

This example is on the sensitivity analysis of the transient displacement and voltage with respect to three kinds of design variables. The structure is shown in Fig. 2. The cross-sectional areas are 3.0E-4 m^2 and the thickness of each piezoelectric piece 0.005 m. The feedback gain coefficients are g = 4.0E6 and h = 4.0E4 for all the bars. The piezoelectric material parameters are C_{33} = 8.807E10 N/m^2, e_{33} = 18.62 C/m^2, $\Xi_{33} = 5.92E-9\,(C/Vm)$, and ρ = 7,600 kg/m^3. First, the structure is subjected to loads P_{8y} = 200.0 N until t = 5.0E-3 s; then, the load are removed. Design variables are the cross-sectional areas A_1 to A_{12}, the displacement feedback gain coefficients h_1 to h_{12}, and the velocity feedback gain coefficients g_1 to g_{12}. The sensitivities of the maximum displacement and electrical voltage with respect to design variables are computed by the sensitivity analysis method (SAM) and compared with the global finite difference method (FDM), see Tables 1, 2, and 3. From these tables, it can be found that the results obtained from the SAM have good agreement with the results of the FDM. Thus, it can be concluded that the sensitivity analysis has a good precision.

6.2 Example 2

This example is on the design optimization of a 20-bar piezoelectric truss system. The structure is shown in Fig. 3. The thickness of each piezoelectric piece is 0.005 m. The cross-sectional areas are: A = 3.0E-4 m^2, $\bar{A}$ = 4.0E-4 m^2, and $\underline{A}$ = 2.0E-4 m^2. The piezoelectric material parameters are the same as in the example 1. The feedback gain coefficients for all the bars are: $g = 1.0E4$, $\bar{g} = 4.0E4$, and $\underline{g} = 0.0$; $h = 1.0E6$, $\bar{h} = 4.0E6$, and $\underline{h} = 0.0$. The bars are identified with two end-node numbers in Table 4. First subjected to loads $P_1 = P_2 =$ 200.0 N until t = 5.0E-3 s; then, the load is removed. The number of the time step is 400 and each time step is 0.0005 s. The maximum displacement occurs in the y direction of the node 9, so the integral displacement J_{d-9y} of the node 9 along y direction is considered as the objective function. According to the different kinds of design variables, the following three cases are computed and optimum results of constraint and objective functions are Table 5. Case 1: design variables are the cross-sectional areas A_1 to A_{20}; the optimum design (Table 5) variables are shown in Table 6 and the CPU time is about 5 min. Because the initial feedback gains are not 0 and J_v is not 0, it is necessary that J_v is selected as constraint function. Case 2: design variables are the displacement feedback gain coefficients h_1 to h_{20} and the velocity feedback gain coefficients g_1 to g_{20}; the optimum results are shown in Table 7 and the CPU time is about 7 min. Because some bars are not necessarily selected as piezoelectric active bars, so some optimum feedback gain coefficients in Table 7 are nearly 0 and also because the structural weight is invariable in optimization procedures and J_w is an invalid constraint. But it is listed in Table 5 only for the convenience of results comparison. Case 3: design variables not only include the cross-sectional areas A_1 to A_{2_0} but also include the displacement and velocity feedback gain coefficients h_1 to h_{20} and g_1 to g_{20}; the optimum results are shown in Table 8 and the CPU time is about 14 min. From the Table 5, it can be found that all the constraints are satisfied, but the optimum objective functions are different for three cases. The objective value of the case 3 is the smallest and the best vibration control

Table 4 The relationship between bar with node number

Bar no.	Node no.	Bar no.	Node no.	Bar no.	Node no.	Bar no.	Node no.
1	1, 3	6	4, 6	11	6, 8	16	9, 10
2	2, 4	7	4, 5	12	7, 8	17	1, 4
3	2, 3	8	5, 7	13	8, 10	18	3, 6
4	4, 3	9	5, 6	14	8, 9	19	5, 8
5	3, 5	10	6, 7	15	7, 9	20	7, 10

Table 5 Summary of the optimum design

		$u(t)$	$V(t)$	J_w	J_v	J_{d-9y}
Initial value		−4.0972E-4	7.8748E1	5.3155E1	4.3196E3	1.5474E-5
Upper bound		4.50000E-4	4.0000E2	5.3160E1	4.3000E3	
Optimum values	Case 1	−3.7723E-4	8.9471E1	5.3160E1	4.3000E3	1.0994E-5
	Case 2	−3.7196E-4	2.7596E2	5.3155E1	4.3000E3	0.6579E-5
	Case 3	−3.2819E4	3.0932E2	5.3160E1	4.3000E3	0.3316E-5

Table 6 Optimum areas of cross section of case 1 (m^2)

Areas	Optimum values	Areas	Optimum values	Areas	Optimum values	Areas	Optimum values
A_1	4.00E-4	A_6	4.00E-4	A_{11}	4.00E-4	A_{16}	2.00E-4
A_2	4.00E-4	A_7	4.00E-4	A_{12}	2.00E-4	A_{17}	3.50E-4
A_3	3.30E-4	A_8	4.00E-4	A_{13}	2.00E-4	A_{18}	3.80E-4
A_4	2.00E-4	A_9	2.00E-4	A_{14}	2.00E-4	A_{19}	2.70E-4
A_5	4.00E-4	A_{10}	2.60E-4	A_{15}	2.00E-4	A_{20}	2.00E-4

Table 7 Optimum displacement and velocity feedback gains of case 2

Displacement gains	Optimum values	Velocity gains	Optimum values	Displacement gains	Optimum values	Velocity gains	Optimum values
h_1	0.00	g_1	4.00E4	h_{11}	2.85E6	g_{11}	3.25E4
h_2	0.00	g_2	4.00E4	h_{12}	0.00	g_{12}	1.25E2
h_3	1.33E6	g_3	2.32E4	h_{13}	2.50E4	g_{13}	0.00
h_4	0.00	g_4	1.25E2	h_{14}	0.00E	g_{14}	0.00
h_5	2.63E6	g_5	3.25E4	h_{15}	0.00	g_{15}	1.25E2
h_6	2.55E6	g_6	3.25E4	h_{16}	1.25E4	g_{16}	0.00
h_7	2.68E5	g_7	2.45E3	h_{17}	1.42E6	g_{17}	2.51E4
h_8	2.85E6	g_8	3.25E4	h_{18}	0.00	g_{18}	1.25E2
h_9	0.00	g_9	1.25E2	h_{19}	0.00	g_{19}	0.00
h_{10}	0.00	g_{10}	0.00E	h_{20}	0.00	g_{20}	1.25E2

Table 8 Optimum areas (m^2), displacement, and velocity feedback gains of case 3

Areas	Optimum values	Dis. gains	Optimum values	Vel. gains.	Optimum values	Areas	Optimum values	Dis. gains	Optimum values	Vel. gains.	Optimum values
A_1	4.00E-04	h_1	1.66E6	g_1	4.00E4	A_{11}	4.00E-4	h_{11}	2.85E6	g_{11}	4.00E4
A_2	4.00E-04	h_2	3.46E6	g_2	4.00E4	A_{12}	2.00E-4	h_{12}	0.00	g_{12}	0.00
A_3	3.50E-04	h_3	0.00	g_3	3.72E4	A_{13}	2.00E-4	h_{13}	3.75E4	g_{13}	3.75E2
A_4	2.00E-04	h_4	0.00	g_4	0.00	A_{14}	2.00E-4	h_{14}	1.96E6	g_{14}	8.63E3
A_5	4.00E-04	h_5	3.46E6	g_5	4.00E4	A_{15}	2.00E-4	h_{15}	0.00	g_{15}	0.00
A_6	4.00E-04	h_6	1.74E6	g_6	4.00E4	A_{16}	2.00E-4	h_{16}	0.00	g_{16}	0.00
A_7	4.00E-04	h_7	0.00	g_7	4.00E4	A_{17}	4.00E-4	h_{17}	0.00	g_{17}	4.00E4
A_8	4.00E-04	h_8	2.85E6	g_8	4.00E4	A_{18}	3.20E-4	h_{18}	9.88E5	g_{18}	2.54E4
A_9	2.00E-04	h_9	0.00	g_9	0.00	A_{19}	2.80E-4	h_{19}	2.11E6	g_{19}	2.54E4
A_{10}	2.60E-04	h_{10}	1.54E6	g_{10}	1.50E4	A_{20}	2.00E-4	h_{20}	1.24E6	g_{20}	8.63E3

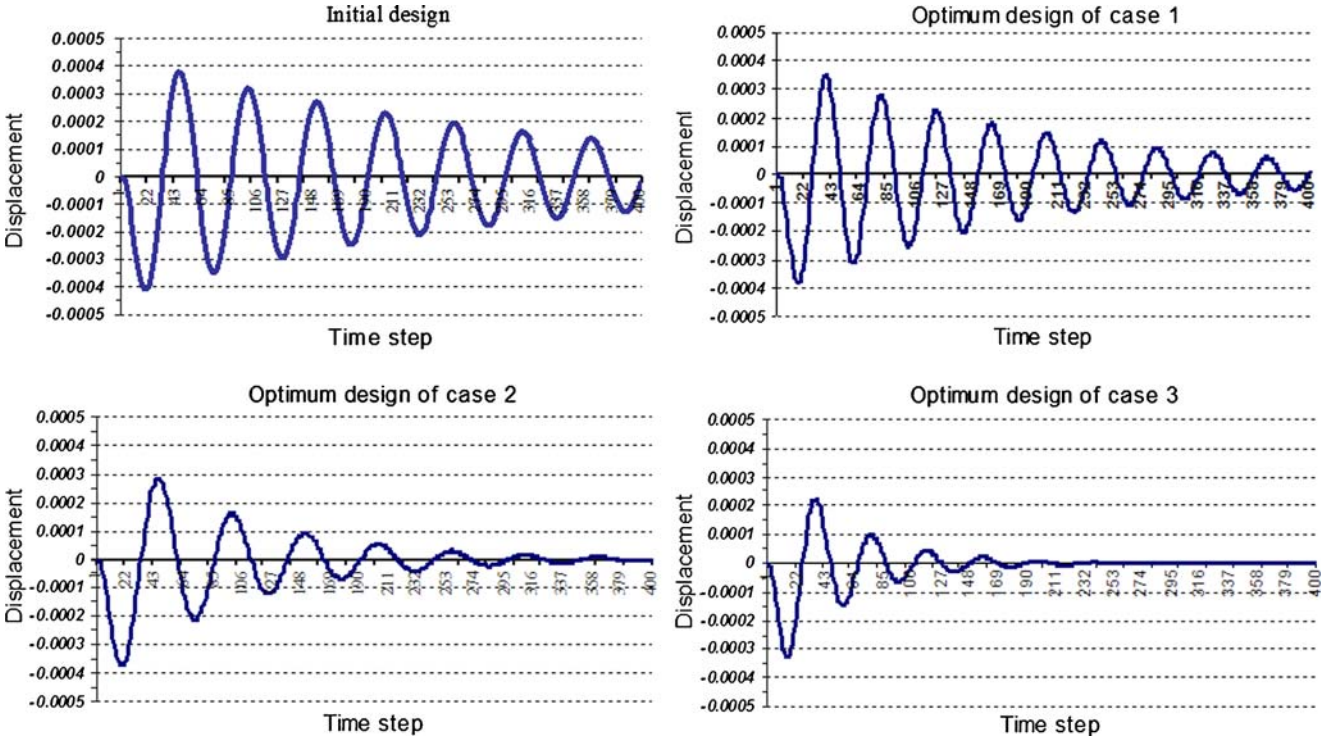

Fig. 4 Displacement response for initial and optimum design

can be obtained by an integrated control–structural design method. Because the cross-sectional areas are selected as design variables in case 1 and case 3 and the maximum transient displacement and electrical voltage do not reach the upper bounds, the optimum areas of most bars in Table 8 are similar to Table 6. Only A_3, A_{17}, A_{18}, A_{19} are a little different. But it can be found that the feedback gains in Table 8 are clearly different from those in Table 7. So the structural variables are useful to find the optimum design in an integrated control–structural design method. Additionally, if the constraint values are modified, for example, decreasing the upper bounds of the maximum transient displacement or electrical voltage, it is possible that optimum areas in case 3 and case 1 are different. In order to compare the optimum results of different cases, the displacement response of node 9 for initial design and optimum design are given in Fig. 4.

6.3 Example 3

This example is on the optimum design of a 72-bar space truss structure. The structure is shown in Fig. 5. The vertical bars and vertical skew bars are composed of piezoelectric material and the other bars are made of conventional material. The cross-sectional areas are 3.0E-3 m^2 and the thickness of each piezoelectric piece 0.005 m. The piezoelectric material parameters are the same as in the example 1 and conventional material parameters are C_{33} = 7.1E10 N/m^2 and ρ = 7,600 kg/m^3. The feedback gain coefficients are g = 4.0E6 and h = 0.0 for all piezoelectric bars. First subjected to loads $P_{2x} = P_{3x} = P_{4x} = P_{5x} = 4.0E5 sin 10.0\pi t$ (N) until t = 0.01 s; then, the load is removed. The number of the time step is 800 and each time step is 0.001 s. The design variables are the cross-sectional areas A_1 to A_{16} and velocity feedback gain coefficients g_1 to g_8, and two end-node numbers in Table 10 identifies the bars relevant with each design variable. The upper and lower bounds of the cross-sectional areas are 3.5E-3 and 2.5E-3 m^2, and the upper

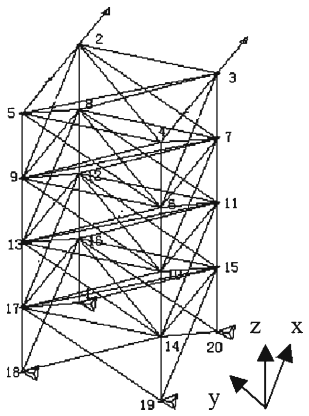

Fig. 5 Seventy-two-bar space truss

Table 9 Summary of the optimum objective and constraints

		$u(t)$	$V(t)$	J_d	J_w	J_v
Initial value		9.379E-3	3.264E2	1.992E-2	6.058E2	1.008E5
Upper bound		9.000E-3	6.000E2	1.000E-2	5.900E2	0.500E5
Optimum values	Case 1	7.988E-3	6.000E2	0.727E-2	5.900E2	0.500E5
	Case 2	8.603E-3	6.000E2	1.000E-2	5.310E2	0.500E5
	Case 3	8.014E-3	6.000E2	1.000E-2	5.900E3	0.375E5

and lower bounds of velocity feedback gain coefficients are 4.0E3 and 0.0. In practical applications, the structure weight, the cost of control, or the dynamic response is probably emphasized partially. According to the different kinds of the objective function, the following three cases are computed. Case 1: The integral displacement J_d of the all nodes is considered as the objective function. The constraint functions include the transient maximum dynamic displacement, the maximum electric voltage, structural weight, and the integral electric voltage J_v. Case 2: The structural weight is considered as the objective function. The constraint functions include the transient maximum dynamic displacement, the maximum electric voltage, the integral displacement J_d, and the integral electric voltage J_v. Case 3: The integral electric voltage J_v is considered as the objective function. The constraint functions include the transient maximum dynamic displacement, the maximum electric voltage, structural weight, and integral displacement J_d. The optimum objective and constraints are seen in Table 9. The optimum design variables are listed in Table 10. The CPU times for Case 1, 2, and 3 are about 20, 23, and 22 min, respectively. From Table 10, the following conclusions can be derived: (1) Although the objective functions and constraint functions are different for different cases, all the constraints are satisfied; (2) after the design optimization, all three performances (J_w, J_d, and J_v) are

Table 10 Optimum value of design variables

Design variables	Node number of bars	Optimum(case 1)	Optimum(case 2)	Optimum(case 3)
A_1	6–4, 7–3, 9–5, 8–2	2.5000E-3	2.5000E-3	2.5000E-3
A_2	10–6, 11–7, 13–9, 12–8	3.5000E-3	2.6116E-3	3.4990E-3
A_3	14–10, 15–11, 17–13, 16–12	3.5000E-3	3.4923E-3	3.4990E-3
A_4	19–14, 20–15, 18–17, 1–16	3.5000E-3	3.4999E-3	3.4990E-3
A_5	5–2, 2–3, 3–4, 4–5	2.5000E-3	2.5000E-3	2.5000E-3
A_6	9–6, 6–7, 7–8, 8–9	2.5000E-3	2.5000E-3	2.5000E-3
A_7	13–10, 10–11, 11–12, 12–13,	2.5000E-3	2.5000E-3	2.5000E-3
A_8	17–14, 14–15, 15–16, 16–17	3.5000E-3	2.5308E-3	3.4990E-3
A_9	7–4, 6–3, 6–5, 9–4, 9–2, 8–5, 7–2, 8–3	2.5000E-3	2.5000E-3	2.5000E-3
A_{10}	11–6, 10–7, 10–9, 13–6, 13–8, 12–9, 11–8, 12–7	2.5000E-3	2.5000E-3	2.5000E-3
A_{11}	15–10, 14–11, 14–13, 17–10, 17–12, 16–13, 15–12, 16–11	3.3871E-3	2.5308E-3	3.3870E-3
A_{12}	9–15, 14–20, 19–17, 18–14, 18–16, 1–17, 20–16, 1–15	3.5000E-3	2.7302E-3	3.4990E-3
A_{13}	5–3, 2–4	2.5000E-3	2.5000E-3	2.5000E-3
A_{14}	9–7, 6–8	2.5000E-3	2.5000E-3	2.5000E-3
A_{15}	13–11, 10–12	2.5000E-3	2.5000E-3	2.5000E-3
A_{16}	17–15, 14–16	2.5000E-3	2.5000E-3	2.5000E-3
g_1	6–4, 7–3, 9–5, 8–2	1.8311E-1	1.1444E-2	3.7231
g_2	10–6, 11–7, 13–9, 12–8	2.0808E-1	1.6830E3	9.1552E-2
g_3	14–10, 15–11, 17–13, 16–12	3.0933E3	2.9048E3	1.6138E3
g_4	19–14, 20–15, 18–17, 1–16	2.3431E3	2.1685E3	2.2892E3
g_5	7–4, 6–3, 6–5, 9–4, 9–2, 8–5, 7–2, 8–3	1.8311E-1	3.3400E-4	3.7231
g_6	11–6, 10–7, 10–9, 13–6, 13–8, 12–9, 11–8, 12–7	1.8311E-1	7.1520E-4	9.1552E-2
g_7	15–10, 14–11, 14–13, 17–10, 17–12, 16–13, 15–12, 16–11	1.8311E-1	1.1444E-2	9.1552E-2
g_8	9–15, 14–20, 19–17, 18–14, 18–16, 1–17, 20–16, 1–15	1.3376E3	1.8570	9.1552E-2

decreased simultaneously; (3) when one performance is selected as the objective function, this performance can be minimized by using the design optimization method effectively. Similarly, optimum areas for all three cases are about the same, but the feedback gains are different. From Table 10, we can find that some optimum feedback gain coefficients are nearly 0. It is obvious these bars are not necessarily selected as piezoelectric active bars.

7 Conclusions

In this paper, an integrated control and structural optimization design model for piezoelectric intelligent truss structures has been presented. The design optimization and sensitivity analysis methods for piezoelectric intelligent trusses with the vibration and control behaviors are proposed with respect to both structural and feedback control variables. The accuracy of sensitivity analysis methods is quite good for the various design variables. It can be concluded that the dynamic response of truss structures can be controlled efficiently by means of regulating electric voltage of piezoelectric active bars. Furthermore an integrated control–structural design optimization can produce better result than structure or control optimization. When the minimization of structural weight or electric energy consumption is considered, how to arrange the cross-sectional areas or the feedback electric voltages is important in practice. Besides, optimum results show that some feedback gain coefficients are nearly 0, therefore the optimal placement of piezoelectric active bars will be an important research issue in the future work. The numerical examples presented here show the effectiveness of the methods.

Acknowledgements The project of research presented in this paper is supported by the National Natural Science Foundation of China (10302006, 10421202 and 10772038). The authors would like to acknowledge these funds support.

References

Bazaraa MS, Shetty CM (1979) Nonlinear programming. Theory and algorithms. Wiley, Hoboken

Chen LW, Lin CY, Wang CC (2002) Dynamic stability analysis and control of a composite beam with piezoelectric layers. Compos Struct 56:97–109

Grandhi RV (1989) Structural and control optimization of space structures. Comput Struct 31(2):139–150

Gu YX, Kang Z et al (1998) Dynamic sensitivity analysis and optimum design of aerospace structures. Int J Struct Eng Mech 6(1):31–40

Guyan RJ (1965) Reduction of stiffness and mass matrices. AlAA J 3(2):380

Hwu C, Chang WC, Gai HS (2004) Vibration suppression of composite sandwich beams. J Sound Vib 272:1–20

Kang YK, Prk HC, Kim JH, Choi SB (2002) Interaction of active and passive vibration control of laminated composite beams with piezoceramic sensors_actuators. Mater Des 23:277–286

Lamberti L, Pappalettere C (2004) Improved sequential linear programming formulation for structural weight minimization. Comput Methods Appl Mech Eng 193:3493–3521

Lin JC, Nien MH (2005) Adaptive control of a composite cantilever beam with piezoelectric damping-modal actuators/sensors. Compos Struct 70(2):170–176

Miler DF, Shim J (1987) Gradient-based combined structural and control optimization. J Guid Control 10(3):291–298

Rao SS, Venkayya VB, Khot NS (1988) Optimization of actively controlled structures using goal programming techniques. Int J Numer Methods Eng 26:183–197

Ray MC, Bhattachanrya R, Samanta B (1994) Static analysis of an intelligent structure by the finite element method. Comput Struct 52(4):617–631

Sun K, Zhang FX (1984) Piezoelectricity. Publishing House of National Defense Industry, Beijing (in Chinese)

Sze KY, Yao LQ (2000) Modeling smart structures with segmented piezoelectric sensors and actuators. J Sound Vib 235(3):495–520

Tzou HS, Gadre M (1989) Theoretical analysis of a multi-layered thin shell coupled with piezoelectric shell actuators for distributed vibration controls. J Sound Vib 132(3):433–450

Wang BP (1991) Minimum-weight design of structures with natural-frequency constraints. Finite Elem Anal Des 7(4):325–329

Wang ZD, Chen SH, Han WZ (1999) Integrated structural and control optimization of intelligent structures. Eng Struct 21:183–191

Yang SH, Ngoi B (2000) Shape control of beams by piezoelectric actuators. AIAA J 38(12):2292–2298